Acta Crystallographica Section B
Structural Science
ISSN 0108-7681

Crystal chemistry and binding of NO_2, SCN and SeCN to Co in cobalamins

Gianpiero Garau,[a] Silvano Geremia,[a] Luigi G. Marzilli,[b] Giorgio Nardin,[a] Lucio Randaccio[a]* and Giovanni Tauzher[a]

[a]Centre of Excellence in Biocrystallography, Department of Chemical Sciences, University of Trieste, Via L. Giorgieri 1, I-34127 Trieste, Italy, and [b]Department of Chemistry, Emory University, Atlanta, Georgia 30322, USA

Correspondence e-mail: randaccio@univ.trieste.it

Received 3 July 2002
Accepted 21 October 2002

Results of the accurate crystal structure determination of NO_2Cbl·2LiCl (1), NO_2Cbl·NaCl (2), NCSCbl (3) and NCSeCbl (4), based on synchrotron diffraction data collected at 100 K, are described. The nitro group in (1) was found to be disordered with two orientations that differ by a rotation of $\sim 60^\circ$ about the Co—NO_2 bond, whereas in (2) the nitro group has only one orientation. The first X-ray structural determination of a cobalamin with a Co—Se bond is reported. Comparison of the axial distances indicates that SeCN has a bond length of 2.384 (3) Å and that the *trans* influence on the Co—N bond is only slightly greater than that of SCN. The crystals of the thiocyanate cobalamin contain both the S- and N-bonded coordination isomers in a 3:2 ratio. The structural features of the Co—S bond in cobalamins are discussed. The crystal chemistry of cobalamins is discussed in terms of packing of roughly spherical molecules. The unit-cell parameters can be used to group the cobalamins' crystal structures in different arrays intermediate between distorted hexagonal close packing and primitive hexagonal arrangements. The structural features of cobalamins, and of cobaloximes that have the same axial fragment as the cobalamins, are reviewed and discussed in terms of the *cis* influence of the equatorial ligand.

1. Introduction

Cofactors of the B_{12}-based enzymes belong to the corrinoid cobalt series. In humans, the cofactors are cobalamins (Cbls), which contain a Co atom that is equatorially coordinated by a corrin ring that possesses seven amide side chains (*a*–*g*) (Fig. 1). Chain *f* connects, through an amide bond, a nucleotide, whose benzimidazole base normally coordinates to Co at the axial position on the α side of the corrin macrocycle. In the Co(II) state, this is the only axial ligand. In the Co(III) state, another axial ligand *X* is coordinated on the β side of the equatorial plane (Fig. 1). These cobalamins are denoted by *X*Cbl. *X* may be either an organic group (*R*), which forms a relatively stable Co—C bond, or a neutral or an anionic inorganic ligand. The two B_{12} cofactors have R = Me (methylcobalamin, MeCbl) and R = 5′-deoxy-5′-adenosyl (AdoCbl), whereas vitamin B_{12} itself has X = CN (CNCbl). All the known reactions of B_{12}-dependent enzymes involve the making and breaking of the Co—C bond. For this reason, the Co—C bond features have been widely investigated (Marzilli, 1999). Because transient non-metallo-organic Cbls with O—, N— or S—cobalt ligands are involved in B_{12} biochemistry, structural studies of these inorganic cobalamins are also of interest. Furthermore, since cobalamin molecules generally crystallize with a large number of water molecules, cobalamins provide a suitable model for a structural study of

the biomolecule–water interactions. In particular, the complex hydrogen-bonding scheme between solvent and amide side chains may be relevant to the formation of the coenzyme–apoenzyme complex and to cobalamin transportation (Savage, 1993). The non-organometallic derivatives are very useful in relating spectral and structural properties (Calafat & Marzilli, 1993).

The large cobalamin molecules have a roughly spherical shape and, as observed by Hodgkin *et al.* (1962), their crystals are built up by the stacking of distorted close-packed layers of *X*Cbl molecules. The layers are packed in such a way as to form large cavities that are filled by the solvent molecules, generally water molecules (Bouquiere *et al.*, 1993). The cavities can be described as comprising a central channel that runs along the crystallographic screw axis (parallel to *x*) and connects to side pockets at intervals defined by the screw axis. This crystal structure has been investigated in depth in the case of AdoCbl [by neutron diffraction analysis (Bouquiere *et al.*, 1994)].

In order to study these aspects of cobalamins, it is important to have as many high-resolution structural data as possible. Because of the large size of the cobalamins and the high number of crystallization water molecules, which are often disordered, structure determinations for these intriguing biomolecules were of low accuracy until 1994. Cobalamin structure determinations with accuracies that are comparable to those obtained for small molecules have only recently become available, thanks to the use of synchrotron radiation coupled with an area-detector (Kratky *et al.*, 1995; Randaccio *et al.*, 1998, 2000) and to the improvement of crystallization techniques (Randaccio *et al.*, 1999). The first Cbl crystal structure with a complete ordered pattern of solvent molecules within the cavities has recently been reported (Randaccio *et al.*, 2002).

With the aim of obtaining further insight into the structural properties and crystal chemistry of inorganic cobalamins, we report the crystal structures at 100 K of NO_2Cbl·2LiCl (1), NO_2Cbl·NaCl (2), NCSCbl (3) and CNSeCbl (4), which we have determined using synchrotron radiation.

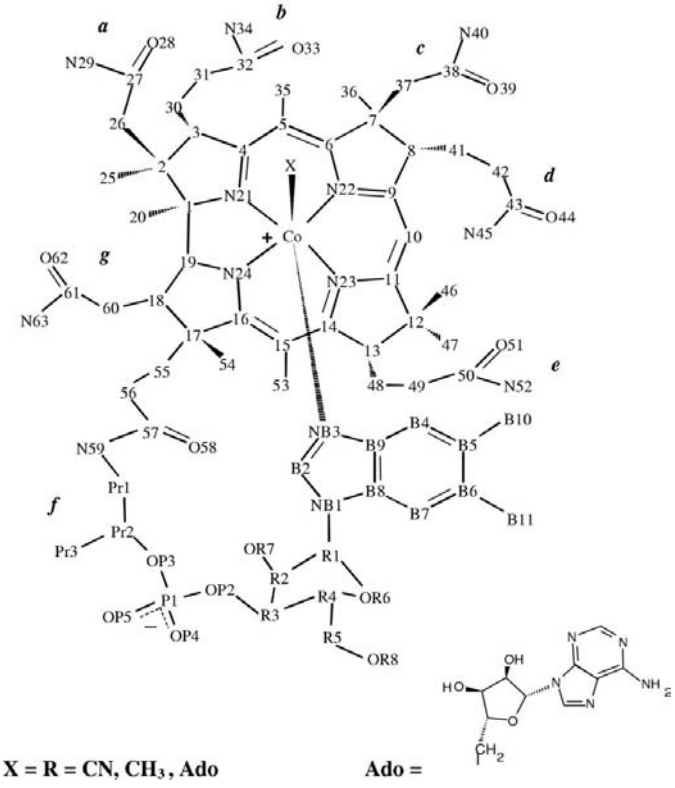

Figure 1
Scheme of the cobalamins with the atom-numbering scheme.

2. Experimental

2.1. Synthesis and crystallization

Compounds (1)–(4) were prepared from commercial high-purity samples of $(H_2O$Cbl$)$Cl obtained from Fluka (stated purity by the manufacturer was greater than 96%). Other reactants were reagent grade and were used without further purification. Crystals of (1) and (2) were prepared by the hanging-drop method of vapour diffusion. Crystallization of (1): 2 µl of an $(H_2O-$Cbl$)$Cl solution at 25 mg ml^{-1} were mixed with 2 µl of a precipitant solution that contained PEG (polyethylenglycol), KNO_2 and LiCl. The droplets were suspended over the same precipitant solution and were allowed to equilibrate at room temperature. Parallelepiped-shaped red crystals appeared in the drop within 4 d with PEG400 25%, KNO_2 0.06 *M* and LiCl 3.0 *M*. Crystallization of (2): parallelepiped-shaped red crystals were obtained by the procedure used for (1), with precipitant solutions that contained PEG400 20%, KNO_2 0.02 *M* and NaCl 3.5 *M*.

To a solution of $(H_2O$Cbl$)$Cl (50 mg) in water (10 ml), 35 mg of potassium thiocyanate or solid potassium selenocyanate were added with stirring. Crystallization of the products [(3) and (4), respectively] was induced by the addition of acetone to the aqueous solutions. During 12 h at room temperature, the solution gradually deposited red crystals of thiocyanato- or selenocyanatocobalamin, which were collected by filtration and air dried.

2.2. X-ray structural determinations

Data collections were carried out at the diffraction beamline of the Elettra Synchrotron (Trieste, Italy). The rotating crystal method, with 0.80 Å monochromatic wavelength and a 30 cm MAR Research imaging plate, was used. Crystals were mounted in a loop and frozen to 100 K with a nitrogen-stream cryocooler. The *MOSFLM* program was used to integrate the diffraction data, and subsequently *SCALA* (Collaborative Computational Project, Number 4, 1994) was used to scale and merge reflections. Bijvoet pairs were not merged and a correction for Co anomalous dispersion was applied. No absorption correction was applied. The structure solution of (1) and (2) used the coordinates of an isomorphous structure as a starting model. The crystal structures of (3) and (4) were solved by direct methods and difference-Fourier techniques. The NO_2 and the SCN groups in (1) and (3), respectively, were

Table 1
Experimental details.

	NO_2Cbl_2·LiCl	NO_2Cbl·NaCl	SCNCbl	SeCNCbl
Crystal data				
Chemical formula	$C_{62}H_{88}CoN_{14}O_{16}P$·-2LiCl·8$H_2O$	$C_{62}H_{88}CoN_{14}O_{16}P$·-NaCl·6.7$H_2O$	$C_{63}H_{88}CoN_{14}O_{14}PS$·-1.7$C_3H_6O$·9$H_2O$	$C_{63}H_{88}CoN_{14}O_{14}PSe$·-$C_3H_6O$·11$H_2O$
Chemical formula weight	1604.27	1554.51	1648.31	1690.59
Cell setting, space group	Orthorhombic, $P2_12_12_1$	Orthorhombic, $P2_12_12_1$	Orthorhombic, $P2_12_12_1$	Orthorhombic, $P2_12_12_1$
a, b, c (Å)	15.387 (5), 22.673 (8), 24.381 (4)	15.912 (5), 22.180 (8), 24.725 (4)	15.683 (15), 22.61 (2), 25.10 (3)	15.660 (15), 22.70 (3), 24.96 (3)
V (Å^3)	8506 (4)	8726 (4)	8902 (16)	8872 (17)
Z	4	4	4	4
D_x (Mg m^{-3})	1.253	1.183	1.230	1.266
Radiation type	Synchrotron	Synchrotron	Synchrotron	Synchrotron
Wavelength (Å)	0.800	0.800	0.710	0.710
μ (mm^{-1})	0.36	0.32	0.31	0.70
Temperature (K)	100 (2)	100 (2)	100 (2)	100 (2)
Crystal form, colour	Prism, red	Prism, red	Prism, red brown	Prism, red brown
Crystal size (mm)	0.4 × 0.2 × 0.2	0.3 × 0.2 × 0.2	0.3 × 0.2 × 0.2	0.4 × 0.3 × 0.2
Data collection				
Diffractometer	Area detector MAR345 image plate	Area detector MAR345 image plate	Area detector MAR345 image plate	Area detector MAR345 image plate
Data collection method	φ scans	φ scans	φ scans	φ scans
No. of measured, independent and observed reflections	17 727, 16 605, 12 394	16 313, 15 335, 13 292	20 288, 19 451, 17 986	17 155, 16 620, 14 415
Criterion for observed reflections	$I > 2\sigma(I)$	$I > 2\sigma(I)$	$I > 2\sigma(I)$	$I > 2\sigma(I)$
R_{int}	0.042	0.025	0.038	0.040
θ_{max} (°)	29.8	29.8	27.1	26.0
Range of h, k, l	$-19 \rightarrow h \rightarrow 19$ $-27 \rightarrow k \rightarrow 27$ $-30 \rightarrow l \rightarrow 30$	$-18 \rightarrow h \rightarrow 18$ $-27 \rightarrow k \rightarrow 27$ $-27 \rightarrow l \rightarrow 27$	$-20 \rightarrow h \rightarrow 20$ $-28 \rightarrow k \rightarrow 28$ $-32 \rightarrow l \rightarrow 32$	$-19 \rightarrow h \rightarrow 19$ $-28 \rightarrow k \rightarrow 28$ $-30 \rightarrow l \rightarrow 30$
Refinement				
Refinement on	F^2	F^2	F^2	F^2
$R[F^2>2\sigma(F^2)]$, $wR(F^2)$, S	0.104, 0.306, 1.21	0.121, 0.336, 1.53	0.071, 0.204, 1.04	0.088, 0.256, 1.04
No. of reflections and parameters used in refinement	16 605, 966	15 335, 918	19 451, 1008	16 620, 1026
H-atom treatment	Mixed	Mixed	Mixed	Mixed
Weighting scheme	$w = 1/[\sigma^2(F_o^2) + (0.2P)^2]$ where $P = (F_o^2 + 2F_c^2)/3$	$w = 1/[\sigma^2(F_o^2) + (0.2P)^2]$ where $P = (F_o^2 + 2F_c^2)/3$	$w = 1/[\sigma^2(F_o^2) + (0.1474P)^2 + 4.9733P]$ where $P = (F_o^2 + 2F_c^2)/3$	$w = 1/[\sigma^2(F_o^2) + (0.1910P)^2 + 6.1134P]$ where $P = (F_o^2 + 2F_c^2)/3$
$(\Delta/\sigma)_{max}$	2.158	1.368	13.889	3.937
$\Delta\rho_{max}$, $\Delta\rho_{min}$ (e Å^{-3})	1.15, −0.92	0.94, −0.91	0.94, −1.13	0.87, −2.12
Flack parameter (Flack, 1983)	−0.08 (2)	−0.05 (2)	0.04 (1)	0.04 (1)

Computer programs used: *SHELXS*97 (Sheldrick, 1997), *SHELXL*97 (Sheldrick, 1997).

found to be disordered and were refined over two orientations. The chain *c* in (2) was found to be disordered over two positions with occupancy factors of 0.7 and 0.3, respectively. In addition to crystallization water molecules, three acetone molecules with occupancy factors of 1.0, 0.45 and 0.25, respectively, were found in (3), whereas one acetone molecule with full occupancy was detected in (4). The full-matrix least-squares technique was used to refine the structures. All the non-H atoms with full occupancy were refined with anisotropic thermal parameters; the remaining non-H atoms were refined isotropically. All H atoms of the cobalamin moiety were placed in idealized positions and refined as riding atoms with the relative isotropic parameters. The H-atom positions of the water molecules with full occupancy were determined with the *HYDROGEN* program (Nardelli, 1999) and then checked (and adjusted if necessary) on the difference-Fourier maps. H atoms of solvent molecules with fractional occupancy were not included.

Calculations were performed with the *SHELXL* programs (Sheldrick, 1997). The crystal data and refinement details are reported in Table 1.[1]

3. Results and discussion

3.1. Molecular structures of (1)–(4)

The crystals of (1) contain two LiCl units per Co atom, as found in other inorganic cobalamins crystallized in the presence of LiCl (Randaccio *et al.*, 2000). The crystals of (2)

[1] Supplementary data for this paper are available from the IUCr electronic archives (Reference: NA0139). Services for accessing these data are described at the back of the journal.

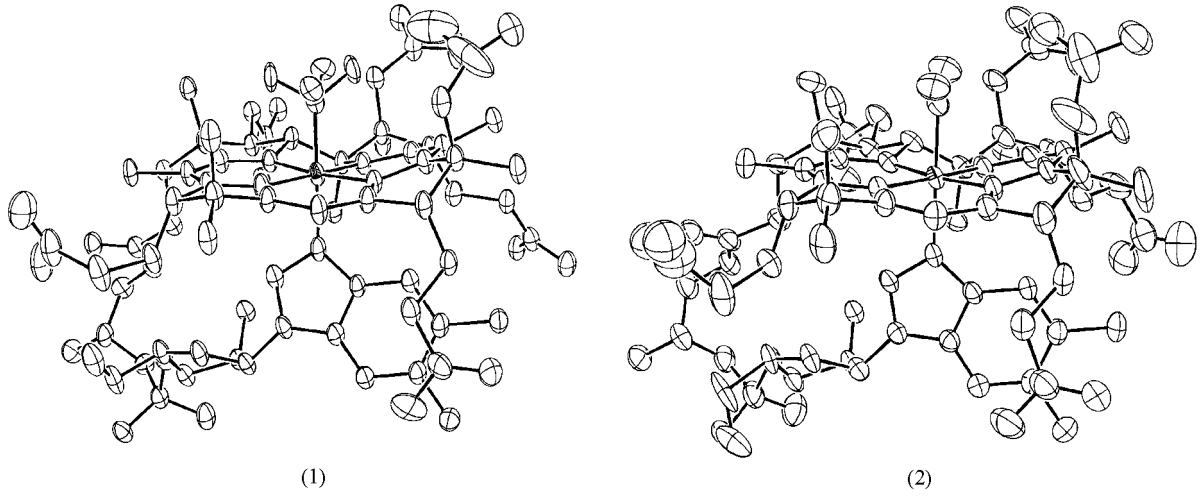

Figure 2
ORTEP drawings of (1) and (2) with 30% probability thermal ellipsoids. The two orientations of the nitro group in (1) are shown. The solvent molecules are not shown for the sake of clarity.

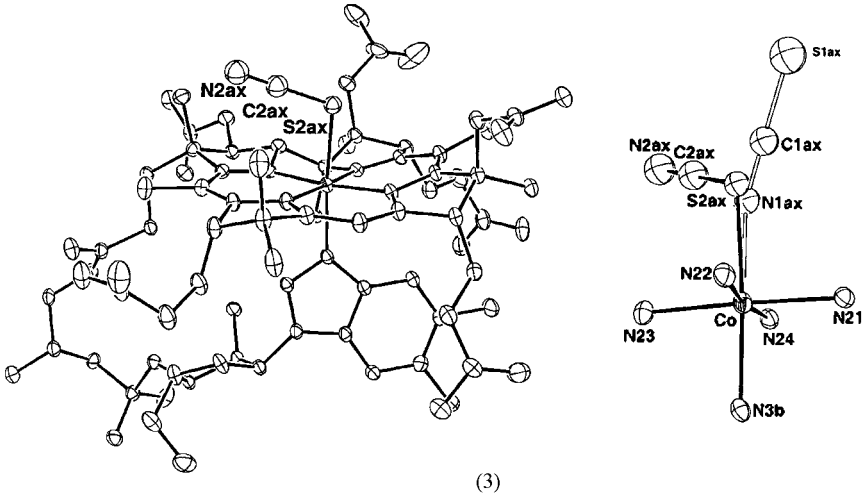

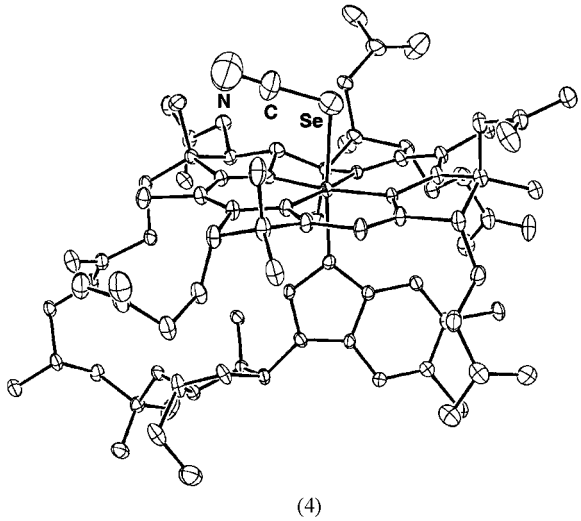

Figure 3
ORTEP drawings of (3) and (4) with 30% probability thermal ellipsoids. The two N and S views of thiocyanate binding are shown in the upper part (right). The solvent molecules are not shown for the sake of clarity.

contain one NaCl unit per Co, as found in CNCbl·KCl (Randaccio *et al.*, 2000). Note that ionic species (which are located in the cavities and interact with the amide side chains) are found inside the crystal only when *X* is a mono-anionic ligand (Cl^-, CN^-, NO_2^-) that is able to form a hydrogen bond with the amide side chain *c* (Randaccio *et al.*, 1998). In fact, we were unsuccessful in including electrolytes by crystallizing, in the presence of alkaline halides, either alkylcobalamins or inorganic cobalamins with neutral (H_2O, thiourea) or dianionic (sulfite) *X* ligands.

The *ORTEP* drawings of (1)–(4) are shown in Figs. 2 and 3. In (1), the axial NO_2 group is disordered in two orientations, which differ by a rotation of $\sim60^\circ$ about the Co—N bond. In one orientation (occupancy factor of 0.6) the NO_2 plane approximately bisects the C1—C19 bond of the five-membered equatorial ring (Fig. 1). In the other orientation (occupancy factor of 0.4), the NO_2 group forms an ONO···N40 hydrogen bond of 2.61 (3) Å and an H···O bond of 1.75 Å with the *c* amide group. In (2), the nitro group has only one orientation. This group forms an ONO···N40 hydrogen bond of 3.06 (2) Å and an H···O bond of 2.20 Å (Fig. 2) with the amido group of chain *c* with an occupancy factor of 0.7 (see §2.2). Both N- and S-bonded coordination isomers are found in (3), as shown

Table 2
Coordination distances (Å) and some coordination bond angles (°) in (1), (2), (3) and (4) with s.u. values in parentheses.

	(1) (X = NO_2)	(2) (X = NO_2)	(3) (X = SCN)	(4) (X = SeCN)
Co—X	1.942 (6)	1.912 (5) 1.94 (1) (N)	2.250 (4) (S)	2.384 (3)
Co—NB3	1.992 (6)	2.014 (5)	1.994 (4)	2.020 (5)
Co—N21	1.873 (5)	1.868 (5)	1.889 (3)	1.889 (5)
Co—N22	1.920 (4)	1.902 (5)	1.920 (3)	1.915 (5)
Co—N23	1.919 (5)	1.900 (5)	1.922 (4)	1.913 (5)
Co—N24	1.894 (5)	1.870 (5)	1.898 (3)	1.898 (5)
N21—Co—N22	90.1 (2)	89.9 (2)	90.4 (1)	90.5 (2)
N21—Co—N24	82.7 (2)	83.0 (2)	83.2 (1)	83.3 (2)
N22—Co—N23	95.9 (2)	96.4 (2)	96.5 (1)	96.5 (2)
N23—Co—N24	91.4 (2)	90.8 (2)	90.1 (1)	89.8 (2)
NB3—Co—X	176.1 (2)	175.2 (2) 176.7 (3) (N)	173.0 (1) (S)	172.5 (1)

in Fig. 3, with occupancy factors of 0.55 and 0.45, respectively. No positional disorder is detected for NB3, as it does not exhibit high thermal parameters. This lack of disorder suggests that thiocyanate exerts a very similar *trans* influence in both coordination modes. In (4), only the Se-bonded isomer is present. No intramolecular hydrogen bond between the axial ligand and the *c* amide chain is detected in (3) and (4), since the *c* amide chain is oriented away from the axial ligand.

The coordination distances and angles in (1)–(4) are given in Table 2 and refer to the numbering scheme of Fig. 1. As expected, the Co–N21 and Co–N24 equatorial distances, which are involved in the Co—N21—C1—C19—N24 five-membered ring, are shorter than the Co—N22 and Co—N23 equatorial distances, which are involved in the Co—N22—C9—C10—C11—N23 chelate ring. The Co—NB3 distances reveal that the SCN and NO_2 groups have a very similar *trans* influence, which is slightly smaller than that of SeCN. To our knowledge, the Co—Se distance of 2.384 (3) Å is the first experimental value so far reported for cobalamins. It is very close to the value of 2.383 Å that was reported for the cobaloxime $[CNSeCo(DH)_2SeCN]^-$ anion (Sumus & Belov, 1970). Cobaloximes $XCo(DH)_2L$, which are simple B_{12} models, are octahedral cobalt(III) complexes in which the equatorial DH ligand is the monoanion of dimethylglyoxime and L is generally a neutral Lewis base (Randaccio, 1999).

3.2. Crystal chemistry of cobalamins

It has been shown (Gruber *et al.*, 1998) that the vast majority of cobalamins that crystallize in the $P2_12_12_1$ space group are isomorphous and can be assigned to four groups (clusters) I–IV, which are characterized by different values of the cell axis ratios *c*/*a* and *b*/*a* (Fig. 4). Crystal-packing analyses show that each cluster corresponds to a different stacking of the distorted close-packing layers of the roughly spherical cobalamin molecules. A typical distorted close-packed layer is sketched in Fig. 5, which shows that each molecule is surrounded by six others in a roughly hexagonal arrangement.

The close-packed layers are similar in all the structures of the clusters, which differ essentially in the way that the layers are stacked (Gruber *et al.*, 1998). If we consider the Co atoms as the centres of the spheres, a typical stacking of the layers, whose mean planes are separated by one-half of the *c* edge of the unit cell, is sketched in the upper part of Fig. 6(*a*). This stacking resembles the well known hexagonal close packing (h.c.p.) of spheres shown in the upper part of Fig. 6(*b*), where each sphere is in contact with another twelve (six in the plane, three in the plane below and three in the plane above) as shown in the lower part of Fig. 6(*b*). The corresponding twelvefold environment about each sphere in the packing of (1)–(4) is shown in the lower part of Fig. 6(*a*). However, in contrast with the h.c.p. arrangement, where all the centres of the spheres in each stacked plane are coplanar, the Co centres of each stacked plane of Fig. 6(*a*) are not coplanar. Therefore, each plane is corrugated, and its 'depth' is measured by the difference, Δz, between the Co centres above and below the plane. Because the planes are along the crystallographic z axis at z = 1/4 and 3/4, $\Delta z = 1/2 - 2z(\mathrm{Co})$, the relative height of the centres, along the crystallographic z axis, is represented by different types of circles in Fig. 6(*a*). The shift between two adjacent layers can be measured by the vector **S** with components $Sx = -2x(\mathrm{Co}) + 1/2$, $Sy = -2y(\mathrm{Co})$, $Sz = 1/2$, where x(Co), y(Co) and z(Co) are the fractional coordinates of Co. The packing in the four clusters differs in **S** and Δz. Typical ranges of Δz, Sx and Sy are given in Table 3, where the corresponding values for the h.c.p. arrangement are also reported for a distance of 15 Å between two adjacent Co centres. This table shows that cluster III exhibits the largest Δz and a packing closer to the primitive hexagonal packing than to h.c.p., as compared with that of the clusters. Since cluster III contains only several AdoCbl structures, which

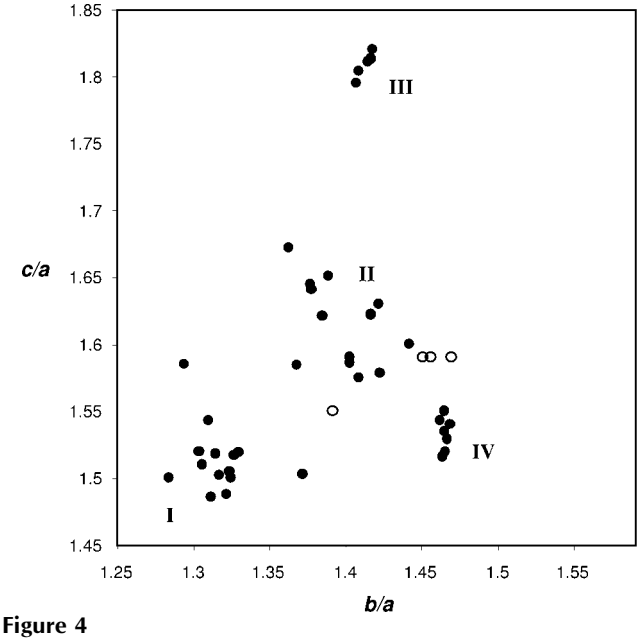

Figure 4
Scatter plot of *c*/*a* *versus* *b*/*a* for cobalamins. Open circles refer to structures reported in the present manuscript, from left to right in the order (2), (3), (4) and (1).

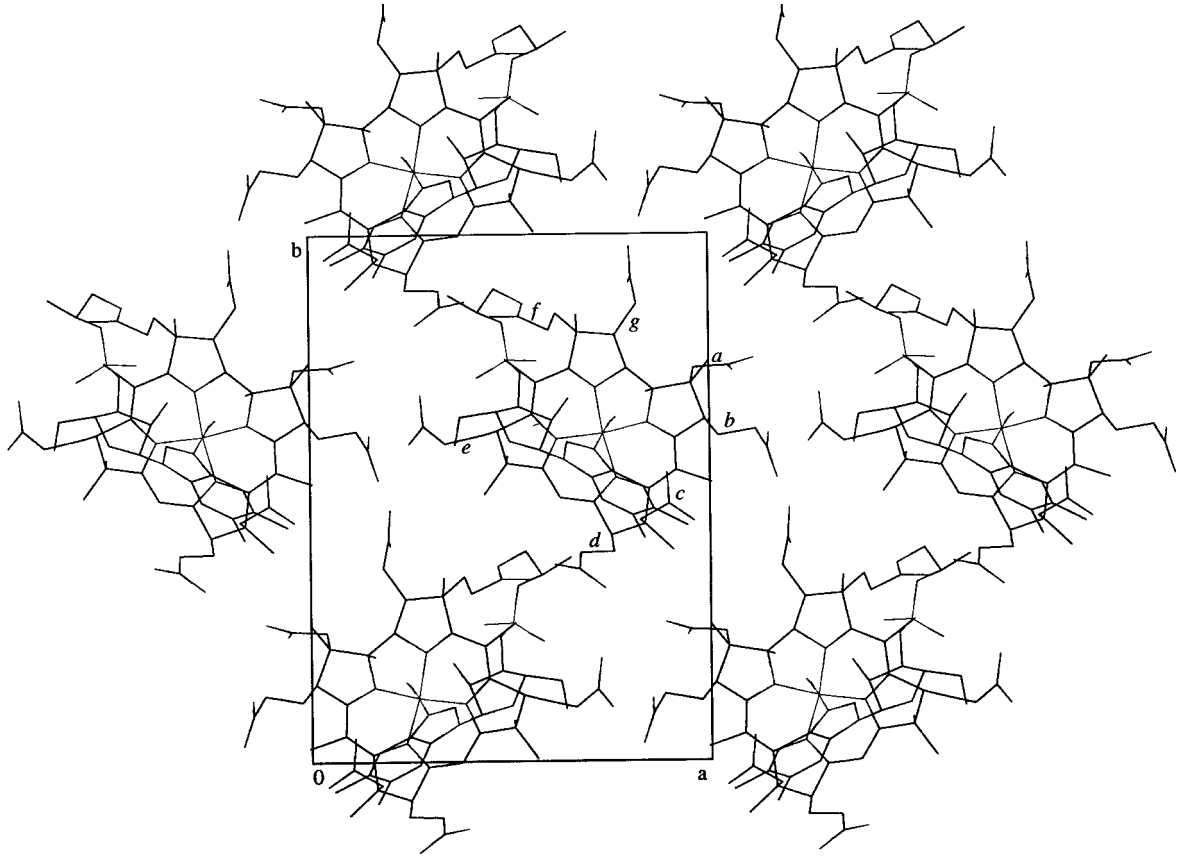

Figure 5
The close-packed plane of cobalamin molecules that is typical of all the crystal structures of cobalamins.

Table 3
Ranges of Δz, Sz, Sy (values in Å) for clusters I–IV, and h.c.p. arrangement (d is the distance between two adjacent centres).

	Δz	Sx	Sy	d
I	1.08, 2.22	−0.44, −0.77	−6.23, −4.331	12.8–16.7
II	0.08, 0.29	−0.49, −0.30	−4.39, −4.14	13.5–16.7
III	2.58, 2.69	−0.56, −0.61	−2.68, −2.95	13.7–15.8
IV	1.12, 1.133	−1.32, −1.38	−4.44, −4.11	12.6–16.8
h.c.p.	0	0	−8.66	15.0

differ by their acetone/water solvent ratio, this difference could be due to the steric influence of the large adenosyl axial ligand.

3.3. Hydrogen-bonding scheme in (1)–(4)

It has been shown (Randaccio *et al.*, 2000) that cobalamins that belong to the same cluster have very similar conformations for all the amide side chains and very similar intra- and intermolecular hydrogen-bond patterns. In particular, cobalamins that belong to clusters I and IV are characterized by a *c* chain conformation such that the amide group is directed towards the *X* axial ligand and forms an intramolecular hydrogen bond with the ligand. In addition, the conformations of the *e* and *f* chains in cobalamins of group IV are arranged in such a way as to form another intramolecular hydrogen bond between the O*R*8 (chain *f*) and O51 (chain *e*). Cobalamins of

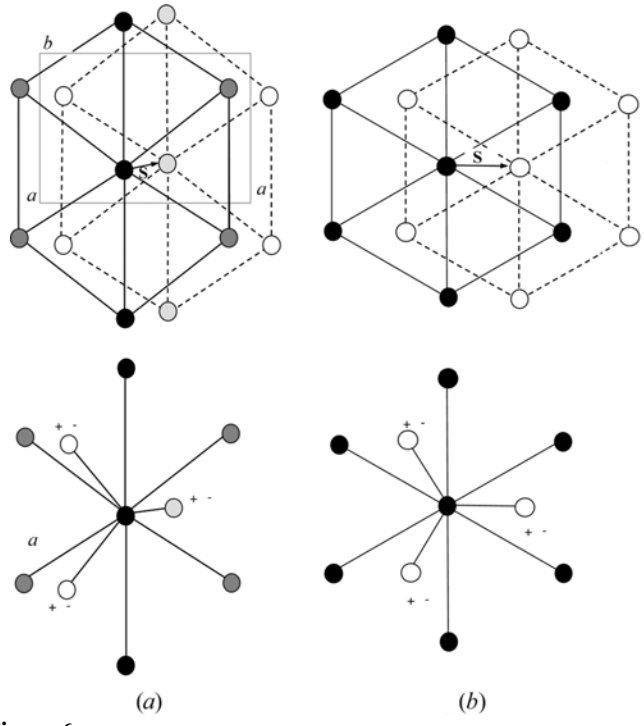

Figure 6
(*a*) Sketch of the stacking along *z* of the close-packed planes in cobalamins (upper) and the distorted twelvefold coordination about each sphere (lower). The unit cell projected along *z* is also shown. (*b*) Stacking of the close-packed planes (upper) and the twelvefold coordination around each sphere (lower) in the hexagonal close packing.

Table 4
Hydrogen bonds and angles in (1)–(4).

Donor (*D*)	Distance (Å)		Angle (°)	
D—H	H···*A*	*D*···*A*	*D*—H···*A*	Acceptor (*A*)
(1)				
N29—H29*A*	2.34	3.138 (11)	151	O44^{i}
N29—H29*B*	2.40	3.277 (8)	172	Cl1
N34—H34*B*	2.39	3.271 (7)	174	Cl1^{ii}
N40—H40*B*	1.75	2.61 (3)	165	O2*X*2
N40—H40*B*	2.55	3.35 (3)	152	O2*X*1
N45—H45*B*	2.48	3.282 (19)	152	OW8*A*
N52—H52*A*	2.15	2.89 (2)	141	OW7^{iii}
N52—H52*B*	2.86	3.692 (14)	158	Cl2
N59—H59	2.31	3.114 (7)	152	OW2^{iv}
N63—H63*A*	2.25	3.025 (9)	148	OW5^{iv}
N63—H63*B*	2.33	3.195 (8)	167	Cl1
O*R*7—H*R*7	1.84	2.698 (5)	180	OW2^{iv}
O*R*8—H*R*8	2.05	2.872 (13)	177	O51
OW1—H1W1	2.17	3.100 (6)	175	OW3^{iv}
OW1—H1W2	1.93	2.863 (7)	173	O58^{v}
OW2—H2W1	1.93	2.847 (7)	165	OW3^{vi}
OW2—H2W2	1.94	2.805 (6)	153	OP4
OW3—H3W1	1.83	2.711 (7)	156	OP5
OW3—H3W2	1.84	2.758 (5)	165	O33^{vi}
OW4—H4W1	2.17	3.083 (4)	166	Cl2^{vii}
OW4—H4W2	1.95	2.835 (7)	157	O33^{viii}
OW5—H5W1	1.79	2.700 (8)	163	O39^{ix}
OW5—H5W2	2.40	3.297 (5)	162	Cl2^{vii}
OW6—H6W1	1.97	2.886 (7)	165	O*R*8^{iii}
OW6—H6W1	2.57	3.131 (5)	119	O*R*6^{iii}
OW6—H6W2	2.47	3.396 (4)	173	Cl1
(2)				
N29—H29*A*	2.17	3.023 (13)	162	O44^{i}
N29—H29*B*	2.62	3.364 (14)	143	OW6
N34—H34*B*	1.88	2.689 (18)	151	OW5
N40I—H4*B*I	2.20	3.061 (16)	164	O2*X*
N45—H45*B*	2.34	3.205 (13)	166	OW4
N52—H52*A*	2.45	3.161 (19)	139	O28^{viii}
N52—H52*B*	2.22	3.04 (2)	154	OW1
N59—H59	1.94	2.802 (13)	168	Cl1
N63—H63*A*	2.23	2.996 (16)	145	O51^{iii}
N63—H63*B*	1.85	2.722 (11)	172	OW5^{i}
O*R*7—H*R*7	1.93	2.766 (6)	171	OW3^{ix}
OW1—H1W1	2.28	3.152 (11)	155	OW2
OW1—H1W2	1.70	2.619 (13)	166	O58
OW3—H3W1	1.89	2.757 (14)	153	Cl1^{x}
OW3—H3W2	1.92	2.786 (9)	152	OP4^{xi}
OW5—H5W1	2.09	2.994 (5)	163	OW6^{ii}
OW7—H7W1	1.54	2.466 (16)	169	O51
(3)				
N29—H29*A*	2.14	2.995 (8)	173	O44^{i}
N29—H29*B*	2.25	3.078 (15)	160	OW8^{i}
N34—H34*A*	1.99	2.807 (12)	159	OW12^{v}
N34—H34*B*	2.05	2.777 (7)	142	OW6*A*
N40—H40*A*	2.10	2.954 (5)	171	OP4^{x}
N40—H40*B*	2.17	2.908 (7)	144	OW5^{x}
N45—H45*A*	2.37	2.89 (4)	119	O2*A*C^{xi}
N45—H45*B*	2.14	3.000 (11)	174	O1*A*C^{xi}
N52—H52*A*	2.10	2.836 (8)	144	O28^{viii}
N52—H52*B*	2.05	2.885 (8)	165	OW1^{vi}
N59—H59	2.06	2.911 (6)	172	OW4
N63—H63*A*	2.15	2.962 (6)	158	O51^{iii}
N63—H63*B*	1.96	2.807 (8)	170	OW6*A*^{i}
O*R*7—H7*R*	1.94	2.758 (5)	176	OW3
O*R*8—H8*R*	2.03	2.811 (12)	159	OW12
OW1—H1W2	2.04	2.809 (7)	138	O58^{iv}
OW2—H2W1	1.78	2.670 (6)	159	O39^{ix}
OW2—H2W2	1.83	2.685 (6)	152	OP4
OW3—H3W1	1.83	2.729 (6)	160	OP5^{iv}
OW3—H3W2	1.87	2.778 (7)	163	OW2
OW4—H4W1	1.89	2.820 (6)	177	OW3
OW4—H4W2	2.06	2.900 (6)	148	O62
OW5—H5W1	2.10	2.908 (7)	144	N40^{ix}
OW6*A*—H6W2	2.17	2.741 (11)	119	OW8
(4)				
N29—H29*A*	2.16	3.023 (10)	167	O44^{i}
N29—H29*B*	2.45	3.168 (17)	139	OW8^{i}
N34—H34*A*	1.97	2.815 (13)	159	OW6
N34—H34*B*	2.02	2.758 (9)	141	OW6*A*
N40—H40*A*	2.08	2.951 (8)	170	OP4^{x}
N40—H40*B*	2.18	2.929 (8)	142	OW5^{x}
N45—H45*B*	2.17	3.043 (14)	174	O1*A*C^{xi}
N52—H52*A*	2.13	2.864 (11)	141	O28^{viii}
N52—H52*B*	2.07	2.937 (11)	167	OW1^{vi}
N59—H59	2.04	2.914 (7)	170	OW4
N63—H63*A*	2.14	2.983 (9)	159	O51^{iii}
N63—H63*B*	1.94	2.811 (10)	170	OW6*A*^{i}
O*R*7—H7*R*	1.93	2.756 (7)	169	OW3
O*R*8—H8*R*	2.20	2.831 (9)	132	OW5
OW1—H1W1	1.99	2.803 (11)	144	OW2
OW1—H1W2	1.94	2.853 (10)	165	O58^{iv}
OW2—H2W1	1.87	2.648 (9)	139	O39^{ix}
OW2—H2W2	1.78	2.697 (10)	166	OP4
OW3—H3W1	1.90	2.737 (8)	148	OP5^{iv}
OW3—H3W2	2.25	2.827 (9)	119	OW2
OW4—H4W1	2.19	2.831 (9)	125	OW3
OW4—H4W2	2.21	2.914 (7)	132	O62
OW5—H5W1	1.95	2.760 (7)	144	OW62^{xii}
OW5—H5W2	2.34	2.831 (9)	112	O*R*8
OW6—H6W3	2.02	2.56 (3)	115	OW14^{xiii}
OW6—H6W4	1.83	2.759 (13)	171	O*R*8^{v}
OW6*A*—H6W2	2.22	2.786 (15)	118	OW8
OW8—H8W1	1.83	2.41 (4)	118	OW61^{ii}

Symmetry codes: (i) $-x, y+\frac{1}{2}, -z+\frac{1}{2}$; (ii) $-x, y-\frac{1}{2}, -z+\frac{1}{2}$; (iii) $-x+1, y+\frac{1}{2}, -z+\frac{1}{2}$; (iv) $x-\frac{1}{2}, -y+\frac{1}{2}, -z+1$; (v) $x-1, y, z$; (vi) $x+\frac{1}{2}, -y+\frac{1}{2}, -z+1$; (vii) $-x+\frac{3}{2}, -y, z+\frac{1}{2}$; (viii) $x+1, y, z$; (ix) $-x+\frac{1}{2}, -y, z+\frac{1}{2}$; (x) $-x+\frac{1}{2}, -y, z-\frac{1}{2}$; (xi) $-x+1, y-\frac{1}{2}, -z+\frac{1}{2}$; (xii) $x+\frac{1}{2}, -y+\frac{1}{2}, z+1$; (xiii) $-x, y-\frac{1}{2}, -z+\frac{3}{2}$.

groups II and III do not form intramolecular hydrogen bonds. Cobalamin (1) has the two typical intramolecular hydrogen bonds of cluster IV, but it has a *c*/*a* ratio larger than that found for this cluster (Fig. 4). Cobalamin (2) has the intramolecular (ONO···N40) hydrogen bond of cluster I but intermolecular hydrogen bonds typical of cluster II. Cobalamins (3) and (4) belong to cluster II.

Intermolecular hydrogen bonds involve the O atoms of the ribosyl phosphate, the amide groups of the side chains and the water molecules, as shown in Table 4. The hydrogen-bond networks in (1) and (2) are similar to those already described in CNCbl·2LiCl and CNCbl·KCl (Randaccio *et al.*, 2000), respectively. However, the bond networks differ from those found in (3) and (4), which are very similar (Table 4), as previously described by Hodgkin *et al.* (1962). This similarity is to be expected because (3) and (4) belong to the same cluster.

3.4. The Co—S bond

Despite the biological importance of glutathionylcobalamin in the conversion of CNCbl to the cofactors (Pezacka, 1993), only a few cobalamins that contain a Co—S axial bond (Randaccio *et al.*, 2002) and only one that contains a Co–

Table 5
Distances Co—X and Co—NB3 in cobalamins and cobaloximes.

Data are from Randaccio *et al.* (2000) if not otherwise stated.

	Cobalamin		Cobaloxime	
	Co—X	Co—NB3	Co—X	Co—Npy
H_2O	1.952 (2)	1.925 (2)	1.916 (3)	1.926 (3)
Cl	2.252 (1)	1.981 (3)	2.229 (1)	1.959 (2)
N_3	1.980 (3)	1.995 (3)	1.950 (2)	1.973 (1)
SCN	2.250 (4)†	1.994 (4)†	2.267‡	2.017‡
NO_2	1.927 (6)†	2.004 (6)†	1.943 (3)	1.985 (2)
SeCN	2.384 (3)†	2.020 (5)†	2.383§	–
$SC(NH_2)_2$	2.300 (2)	2.032 (5)	2.273¶	2.012¶
CN	1.886 (4)	2.041 (3)	1.937 (2)	1.995 (2)
γ–Glut-Cys	2.267 (2)††	2.049 (6)††	2.286‡‡	1.989 (5)‡‡
SO_3	2.231 (1)	2.134 (4)	2.225 (2)	2.042¶
Me	1.979 (4)	2.162 (4)	1.998 (5)	2.068 (3)
CHF_2	1.949 (8)	2.187 (7)	1.948 (5)	2.040 (5)
Ado	2.030 (3)§§	2.237 (3)§§	2.015 (2)¶¶	2.072 (2)

† Present work. The mean value is given for NO_2Cbl. ‡ Phthalocyaninato equatorial ligand (Hedtmann-Rein *et al.*, 1987). § Sumus & Belov (1970). ¶ Calculated values from aniline analogues (Bourshtein *et al.*, 1975; Simonov *et al.*, 1979). †† Suto *et al.* (2001). ‡‡ Values for MeS cobaloxime. The Co—S bond is calculated (Randaccio *et al.*, 1999). §§ Unpublished results from this laboratory. ¶¶ X = ribosyl.

thiolate bond, with X = γ-glutamylcysteinyl (γ-Glut-Cys; Suto *et al.*, 2001), have been structurally characterized. The Co—S bond length (Table 5) increases in the order

$$SO_3^{2-}[2.231\,(1)\,\text{Å}] < NCS^{-}[2.250\,(4)\,\text{Å}] < \gamma\text{-Glut-Cys}^{2-}[2.267\,(2)\,\text{Å}] < (NH_2)_2CS[2.300\,(2)\,\text{Å}].$$

This trend seems to reflect in part the electrostatic charge of the axial ligand and follows the increase of the positive charge on Co that is found for the simple corrin analogues by density functional theory (DFT) calculations (Randaccio *et al.*, 2002). The trend of the increasing Co—NB3 distance is

$$NCS^{-}[1.994\,(4)\,\text{Å}] < (NH_2)_2CS[2.032\,(5)\,\text{Å}] < \gamma\text{-Glut-Cys}^{2-}[2.049\,(2)\,\text{Å}] < SO_3^{2-}[2.134\,(4)\,\text{Å}],$$

which reflects the σ-donating ability of the X ligand. This trend is consistent with the decreasing positive charge that is calculated for Co (Randaccio *et al.*, 2002). The above trends give an example of a 'regular' *trans* influence, which occurs when the Co—X bond shortens and the Co—NB3 bond lengthens as a result of an increase in the σ-donating ability of X. In contrast, the 'inverse' *trans* influence was observed in alkylcobalamins (Randaccio *et al.*, 2002) and alkylcobaloximes (De Ridder *et al.*, 1996), in which the Co—C and Co—N axial bonds are both lengthened when the σ-donating ability of R increases.

3.5. Comparison between cobalamins and cobaloximes

Available axial distances in cobalamins (with s.u. values $\leq$ 0.01 Å) and cobaloximes with L = pyridine (py) are given in Table 5. We have shown (Randaccio *et al.*, 2000) that for several X ligands the Co—X and Co—N axial distances in cobalamins are almost linearly related to the axial Co—X and Co—N distances in cobaloximes, respectively. These fairly good linear relationships permitted evaluation of the Co—S and Co—NB3 distances in a thiolatecobalamin, which were not experimentally determined at that time (Polson *et al.*, 1997). The calculated values (Co—S = 2.26 Å; Co—NB3 = 2.04 Å) were in excellent agreement with those recently determined in γ-Glut-Cys Cbl [Co—S = 2.267 (2) Å; Co—NB3 = 2.049 (6) Å] (Suto *et al.*, 2001).

In addition, the fairly good linear regression of the Co—NB3 distances against the Co—py distances gave a slope of 2.00 (2) (r^2 = 0.938), which indicates that the transmission of the *X trans* influence is more effective in cobalamins than in cobaloximes. This increased transmission arises because the electronic *cis* influence of the corrin ligand is significantly greater than the *cis* influence of the $(DH)_2$ ligand grouping. This larger *cis* influence in cobalamins and comparisons with other physicochemical properties suggest a greater electron density on Co in cobalamins than in cobaloximes. A fairly good linear regression between the Co—X distances in cobalamins and in cobaloximes gave a slope of 1.07 (9) (r^2 = 0.949). However, an outlying point found for X = CN was attributed to a greater π back-donation from Co to CN in CNCbl than in the cyanocobaloxime (Randaccio *et al.*, 2000). Another outlying point was found for $X = NO_2$ when preliminary data of NO_2Cbl were used. Present results establish that the point is not an outlier.

However, further analysis of the data shows that the Co—X distances can in the first instance be sorted into three groups: the first with essentially weak *trans*-influencing groups [H_2O, N_3, $SC(NH_2)_2$, Cl], where the Co—X bond length in cobalamins is significantly longer than that in cobaloximes; the second with relatively strong *trans*-influencing ligands (Ado, SO_3, SeCN, CHF_2, NO_2, SCN, thiolate, Me), where the Co—X distances in cobalamins and cobaloximes differ slightly; and the third with the good π-bonding acceptor ligand (CN), where the Co—X distance in cobalamins is significantly shorter. This pattern is illustrated in Fig. 7, where the differences Δ between the Co—X distances in cobalamins and cobaloximes are reported. The differences are markedly positive on the left-hand side, slightly positive or negative in

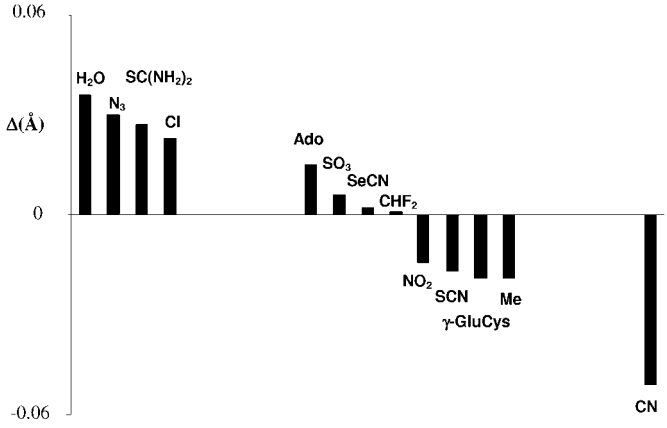

Figure 7
Δ (Å) is the difference between the Co—X distances in cobalamins and the corresponding Co—X distances in cobaloximes. The horizontal spacing has no particular chemical meaning.

the middle, and markedly negative on the right-hand side of Fig. 7. This analysis clearly agrees with the aforementioned better transmission of the *trans* influence in cobalamins than in cobaloximes. In fact, the Co—*X* distances for *trans*-influencing ligands that are weaker than benzimidazole are lengthened in cobalamins with respect to cobaloximes (first group), whereas for *trans*-influencing *X* ligands that are stronger than benzimidazole the Co—*X* bond is almost unaffected (second group). Finally, the greater electron richness of Co in cobalamins (Randaccio *et al.*, 2000) enhances the π back-donation to CN with respect to that in cobaloximes and provokes the relative shortening of the Co—*X* distance.

We thank the Ministero dell'Istruzione, Università e Ricerca (MIUR, Roma) (PRIN MM03185591) and Consiglio Nazionale delle Ricerche (CNR), Agenzia 2000, for financial support.

References

Bouquiere, J. P., Finney, J. L., Lehmann, M. S., Ridley, P. F. & Savage, H. F. J. (1993). *Acta Cryst.* B**49**, 79–89.

Bouquiere, J. P., Finney, J. L. & Savage, H. F. J. (1994). *Acta Cryst.* B**50**, 566–578.

Bourshtein, I. F., Simonov, Y. A., Shchedrin, B. M., Malinovskii, T. I. & Shafranskii, V. N. (1975). *Dokl. Akad. Nauk SSSR*, **222**, 83–85.

Calafat, A. M. & Marzilli, L. G. (1993). *J. Am. Chem. Soc.* **115**, 9182–9190.

Collaborative Computational Project, Number 4 (1994). *Acta Cryst.* D**50**, 760–763.

De Ridder, D. J. A., Zangrando, E. & Burgi, H. B. (1996). *J. Mol. Struct.* **374**, 63–83.

Flack, H. D. (1983). *Acta Cryst.* A**39**, 876–881.

Gruber, K., Jogl, G., Klintsher, G. & Kratky, C. (1998). *Vitamin B_{12} and B_{12}-Proteins*, edited by B. Kräutler, D. Arigoni & B. T. Golding, pp. 335–348. Weinheim: Wiley-VCH.

Hedtmann-Rein, C., Hanack, M., Peters, K., Peters, E. M. & Von Schnering, H. G. (1987). *Inorg. Chem.* **26**, 2647–2651.

Hodgkin, D. C., Lindsay, J., Sparks, R. A., Trueblood, K. N. & White, J. G. (1962). *Proc. R. Soc. London Ser. A*, **266**, 494–499.

Kratky, C., Färber, G., Gruber, K., Deuter, Z., Nolting, H. F., Konrat, R. & Kräutler, B. (1995). *J. Am. Chem. Soc.* **117**, 4654–4670.

Marzilli, L. G. (1999). *Bioinorganic Catalysis*, edited by J. Reedijk & E. Bouwman, pp. 423–500. New York: Marcel Dekker.

Nardelli, M. (1999). *J. Appl. Cryst.* **32**, 563–571.

Pezacka, E. H. (1993). *Biochim. Biophys. Acta*, **1157**, 167–177.

Polson, S. M., Hansen, L. & Marzilli, L. G. (1997). *Inorg. Chem.* **36**, 307–313.

Randaccio, L. (1999). *Comments Inorg. Chem.* **21**, 327–376.

Randaccio, L., Furlan, M., Geremia, S. & Slouf, M. (1998). *Inorg. Chem.* **37**, 5390–5393.

Randaccio, L., Furlan, M., Geremia, S., Slouf, M., Srnova, I. & Toffoli, D. (2000). *Inorg. Chem.* **39**, 3403–3413.

Randaccio, L., Geremia, S., Nardin, G., Slouf, M. & Srnova, I. (1999). *Inorg. Chem.* **38**, 4087–4092.

Randaccio, L., Geremia, S., Stener, M., Toffoli, D. & Zangrando, E. (2002). *Eur. J. Inorg. Chem.* pp. 93–103.

Savage, H. F. J. (1993). *Water and Biological Macromolecules*, edited by E. Westhof, pp. 3–44. London: MacMillan.

Sheldrick, G. M. (1997). *SHELXL*97. *SHELXS*97. University of Göttingen, Germany.

Simonov, Y. A., Botoshansky, M. M., Ablov, A. V., Istru, L. N., Syrtova, G. P. & Malinovskii, T. I. (1979). *Sov. Phys. Crystallogr.* **24**, 274–280.

Sumus, I. D. & Belov, N. V. (1970). *Dokl. Akad. Nauk SSSR*, **333**, 193–194.

Suto, R. K., Brasch, N. E., Anderson, O. P. & Finke, R. G. (2001). *Inorg. Chem.* **40**, 2686–2692.